NRIAG JOURNAL OF ASTRONOMY AND GEOPHYSICS
2021, VOL. 10, NO. 1, 183–201
https://doi.org/10.1080/20909977.2021.1900527

ARTICLE

OPEN ACCESS Check for updates

Combined geophysical and geotechnical investigation of pavement failure for sustainable construction of Owo-Ikare highway, Southwestern Nigeria

Omowumi Ademila

Department of Earth Sciences, Adekunle Ajasin University, Akungba-Akoko, Nigeria

ABSTRACT

Very low frequency electromagnetic (VLF-EM) and electrical resistivity methods involving 54 Schlumberger Vertical Electrical Sounding (VES) and 2-D geoelectrical resistivity imaging using dipole-dipole array were utilised along unstable (US) and stable sections (SS) of Owo-Ikare highway to establish causes of its persistent failure. Engineering evaluation of eighteen soil samples from test pits excavated on selected US and SS were investigated. VLF-EM models, geoelectric sections and 2-D resistivity structures revealed existence of conductive subsurface structures, suspected weak zones beneath the US. The road pavement is constructed on poor clayey subgrade with low resistivity values (<100 Ohm-m) which precipitate instability of the highway. Subgrade soils below US have poor geotechnical properties characterized by high moisture content, liquid limit (43.6–63.8% and 20.1–25.2%), plasticity index (13.4–34.4% and 6.5–8.3%), percentage fines (40–67% and 28–30%), A-7-5 to A-7-6 clayey soils, high linear shrinkage (>10%), low compacted density, low CBR, volume changes (Mv) and impervious soils against those of SS. . Thus, deep-weathering, fractured bedrock, uneven bedrock topography with subsurface structures, water-saturated clayey subgrade and unsuitability of the soils for subgrade and subbase road construction are responsible for instability of the road. Replacement of soil beneath the unstable sections and effective drainage enhances its stability.

ARTICLE HISTORY
Received 21 October 2020
Revised 10 February 2021
Accepted 4 March 2021

KEYWORDS
Geophysical investigation; geotechnical properties; pavement failure; owo-Ikare highway; sustainable roads

1. Introduction

Roads are essential in trade and transportation system globally and serve as links between towns, states and countries. In Africa, roads are links to access education, health and social services. Socio-economic development of a country depends on its transportation network. Thus, soils on which roads are constructed determine its stability and proper usage. Currently, more than half of the major roads in Nigeria are in deplorable state and consistent road maintenance are ineffective. Rehabilitation of roadways has constituted some financial burden to the various tiers of government. Road instability is associated to road usage, maintenance, poor construction materials and practices without regards to the subsoil on which the roads are built (Ademila 2018). Geophysical and geotechnical investigations are integral part of extensive engineering-geological survey that are useful in subsurface characterisation of a complex geological setting. Geophysics applications in highway and foundation studies have been tremendous especially in the mapping of underlying geological setting and subsurface structure (Ademila 2015). The non-recognition of geologic factors has led to many roads and highway pavement instability in the country. Most structural failures can be attributed to inadequate know-how of physical and geologic characteristics of subsoil materials used in construction. Olayinka et al. (2007) used geophysical methods in investigation of structural failures in Nigeria, reported that poor subbase materials and poor compaction during construction account for the failure of rigid pavements in Nigeria. Adeyemi and Oyeyemi (2000) also investigated the failed sections of Lagos-Ibadan expressway, southwestern, Nigeria using geotechnical survey, concluded that soils beneath the failed sections are geotechnically more stable than those beneath stable sections. They identified mechanical properties as not the only means of determining stability of road pavements and emphasised the role of geotechnical properties of subsoil in road stability. The characteristics of soil determine its performance in engineering construction works (Ademila 2018). Most roads in the country have not met national/international standards of stability thus, their failure within a short span. Ademila (2017) emphasised documentation of geotechnical data in pavement design and construction of roads as reference in rehabilitation and construction of sustainable roads. The need to improve the design of roads has prompted this study due to continuous failure of highways in different geologic settings of Nigeria. This study was carried out on Owo-Ikare highway because

CONTACT Omowumi Ademila omowumi.ademila@aaua.edu.ng Department of Earth Sciences, Adekunle Ajasin University, Akungba-Akoko, Nigeria

of its persistent failure despite reconstruction works over the years. Record of geological, geophysical and geotechnical data upon which this road was constructed were scarce. The Owo-Ikare highway is the major link from southwestern Nigeria to the Federal Capital Territory (Abuja). This study is aimed at characterising the subsurface geological condition of the area upon which the road is constructed by integrating geophysical and geotechnical investigations for details on nature of subsoil and subsurface geologic disposition. This is intended to establish cause(s) of persistent failure of this road and recommend lasting solutions for sustainable highway.

2. Description and geology of the study area

Owo-Ikare road is located in the North Senatorial district of Ondo State, Nigeria. It is between latitudes 7° 10′ N and 7° 35′ N and longitudes 5° 30′ E and 5° 50′ E (Figure 1). The area falls within the tropical rain forest region of southwestern Nigeria, characterised by rainy and dry seasons with average rainfall of over 1,500 mm per annum. The broad vegetation of the area is of the rain forest type. The area is characterised by uniform temperature of 27°C and over 70% relative humidity. The road stretches to about 65 km. It shares border with Ido-Ani to the south east, Ikaram-Akoko to the north, Emure-Ekiti to the south west and Akure to the south. The topography is gently undulating, varies from flat terrain to low lands and hilly terrain with elevation above 345 m above sea level (Oluwafemi and Oladunjoye 2013).

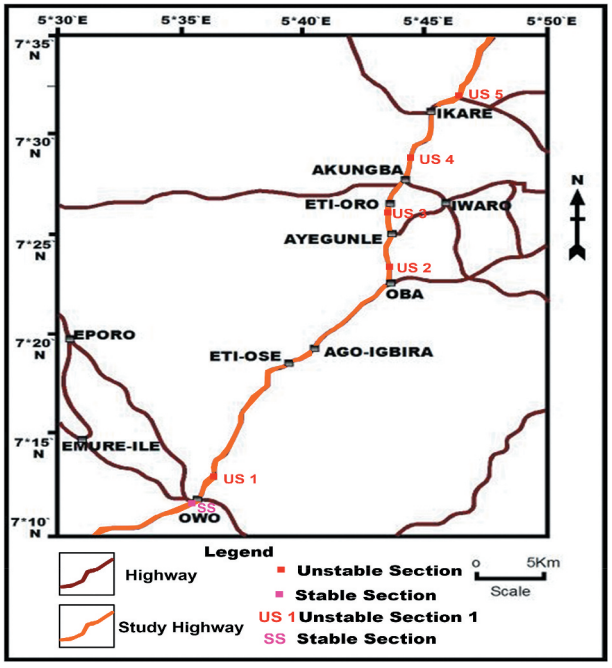

Figure 1. Location map showing Owo-Ikare highway and its environs.

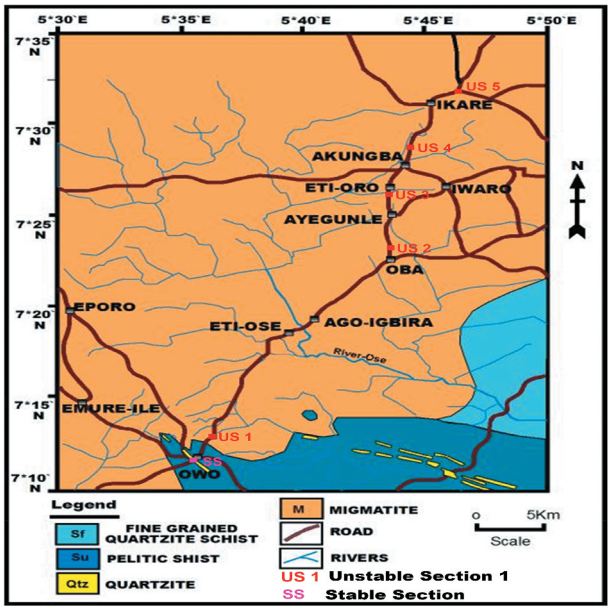

Figure 2. Geological map of the Owo-Ikare highway, Southwestern Nigeria.

The area of study lies within the Precambrian basement geological setting of southwestern Nigeria. It is underlain by the migmatite-gneiss-quartzite complex characterised by migmatite gneiss, granite gneiss, grey gneiss and quartzite (Rahaman 1989). Migmatite gneiss is the dominating rock unit in the area with patches of quartzite (Figure 2). Pegmatites are bounded with the migmatite gneiss as an intrusion. Two varieties of granite gneiss are found in the study area; biotite rich gneiss and banded gneiss. Based on texture, different types of grey gneiss are observed, but the medium-grained rock with regular and persistent banding of varying thickness is recognised. The major rivers draining the area are: Rivers; Alatan, Ogbese, Awara, Ako, Agbo, Isakare, Ose and their major tributaries. They dominate the drainage system of the study area in a dendritic pattern (Ademila 2019). The major aquiferous zones of the area are derivative from weathered rocks and fractured basements beneath the weathered layer from which residents derived water for use through hand dug wells. The range from 3.23 to 10.93 m in depth of the wells suggests shallow water table of the area, which contribute to the failure of the road. The nearness of the aquiferous system to the surface in the study area poses threat to subsoil and civil engineering structures constructed on it (Ademila 2019).

3. Materials and methods

This is a study of thorough geological mapping exercise to determine the lithological units of the area and to characterise unstable and stable sections of the highway. Six geophysical traverses with length varying between 300 and 500 m were established parallel to

five major unstable sections; Owo (US 1), Oba-Akoko (US 2), Etioro-Akoko (US 3), Akungba-Akoko (US 4), Ikare-Akoko (US 5) and one stable section (SS) of the road pavement within the study area. The end of the first 500 m from Owo represents the stable section of the road as deterioration is not yet visible. Traverses were set out at each location parallel to the roadway, cutting across the unstable and stable sections of the highway. Combined geophysical techniques using Very low frequency electromagnetic (VLF–EM) and electrical resistivity methods utilised vertical electrical sounding (VES) and 2-D electrical resistivity imaging using dipole-dipole array were employed along the unstable and stable sections of the highway. VLF–EM survey was carried out beside the highway sections with station to station distance of 10 m with ABEM WADI portable VLF equipment. At each station, real and imaginary components of this VLF–EM were measured. The real component data were thereafter processed. Data were filtered to enhance the signal and make tilt-angle crossovers easier to identify. The VLF–EM results were presented as inverted pseudosections obtained by using KH Filt software (Pirttijarvi 2004). Electrical resistivity method involves measurement of electrical resistance with two pairs of electrode (current and potential electrodes). Electric current is applied between two outer current electrodes, while potential difference is passed across two inner potential electrodes with the resultant electrical resistance measured. Information about subsurface lithology can be derived from varying the electrode separation (Koefoed 1979). VES measurements determine the vertical deviation of geoelectric parameters with respect to depth at each station while the dipole-dipole survey determines lateral and vertical variation in ground apparent resistivity beneath each traverse. In Schlumberger array, distance between the current electrodes is bigger than the distance between the potential electrodes with expansion of current and potential electrodes about a fixed centre. The half of total spread (AB/2) ranges from 1 to 150 m. Sounding points were set up at 50 m interval along each traverse. Fifty-four (54) sounding stations were occupied along the failed sections and stable section using ABEM SAS 1000 terrameter. The apparent resistivity (ρa) were plotted against AB/2 on a log-log paper and presented as field curves. The acquired data was qualitatively interpreted by thoroughly examining the field curves and quantitatively interpreted by partial curve matching (Koefoed 1979) using master curves (Orellana and Mooney 1966) with appropriate auxiliary graphs (Zohdy 1965; Keller and Frischnecht, 1966) to get initial values of geoelectric parameters (resistivity and thickness) of subsurface layers at each VES location. Iteration modelling technique which was the concluding phase of the interpretation was performed using WinResist (Vander-Velpen, 2004). The values of resistivity and thickness were used to construct geoelectric sections. 2-D electrical resistivity imaging using dipole-dipole configuration were employed along the established traverses. Inter-electrode spacing of 10 m was adopted with an expansion factor, n, of 1–5. In dipole-dipole array, four electrodes are used but they do not necessarily occupy position along a common line. The current dipole is separated from the potential dipole, the distance in-between each dipole is short while separation between the two pairs is considerably large. For greater depth of penetration, distance from the current dipole to the potential dipole is increased. The acquired apparent resistivity values were inverted with the aid of Dipro for Windows (2001) and shown as 2-D subsurface resistivity structures using an iterative smoothness-constrained least square inversion.

Eighteen soil samples were obtained from varying locations along Owo-Ikare road based on interpretation results of VES and 2-D subsurface resistivity structures. The soil samples were collected at depths of 0.5–1.5 m from test pits excavated on purposively selected five Unstable Sections (US) and one Stable Section (SS) to ensure actual representation of the subsoil beneath the road pavement. Collection of samples in the study area was in orderly manner. Coordinates and elevation of each of the sampling point was taken with a global positioning system (GPS). Labelled soil samples in sealed polythene bags were taken to the laboratory for analysis and their moisture contents were immediately determined. These soil samples were air dried for 14 days, after which their lumps were softly grounded. Index property tests (consistency limits, linear shrinkage, specific gravity and grain size distribution) and engineering property tests (compaction, California bearing ratio (CBR), triaxial compression, consolidation and permeability) were conducted on the soil samples. The Atterberg limits conducted on these soil samples were in accordance with ASTM D (2017), while other tests were performed on the soils in order of British Standard Methods for civil engineering purposes British Standard (BS) 1377, (1990) and ASTM Standard D1557 (2009).

4. Results and discussion

4.1. Geophysical results

The Karous-Hjelt 2D models give the pictorial distribution of subsurface geologic features. Varying conductive features in different directions were observed on the sections. The identified conductive zones (green to red) delineated the existence of subsurface linear features interpreted as fault/fracture zones and sheared zones within the bedrock. These subsurface conductive features are distinctive zones of weakness precipitating failure of the road as

a result of its contribution to rock instability in a complex geological setting (Ademila et al. 2020). These conductive zones serve as possible sites for groundwater development but cause foundation failure of civil engineering works as a result of its wetness (Ademila et al. 2020). Geophysical evaluation of soil profiles in a complex geological setting requires an in-depth knowledge of its geoelectrical parameters (Telford et al. 1990). Processed electrical resistivity values are displayed as sounding curves, geoelectric sections and 2-D resistivity structures. Six type of curves were achieved from the study; H, AA, A, KH, HA and HK curve types as illustrated in Figure 3 and Table 1. The HA-curve type dominates with percentage frequency of 66.67%. Geoelectric sections which represent geologic sequence mapped with respect to depth are constructed from the quantitative interpretation of the sounding curves (Figure 4b – 9b). Results from the electrical resistivity method showed the distribution of resistivity in the study area. Generally, the geoelectric sections in Figure 4b – 9b show four lithological layers; the topsoil, weathered basement, partially weathered/fractured layer and fresh bedrock. Suitability of subsoil for civil engineering construction works was assessed from the distributed layer resistivity, as

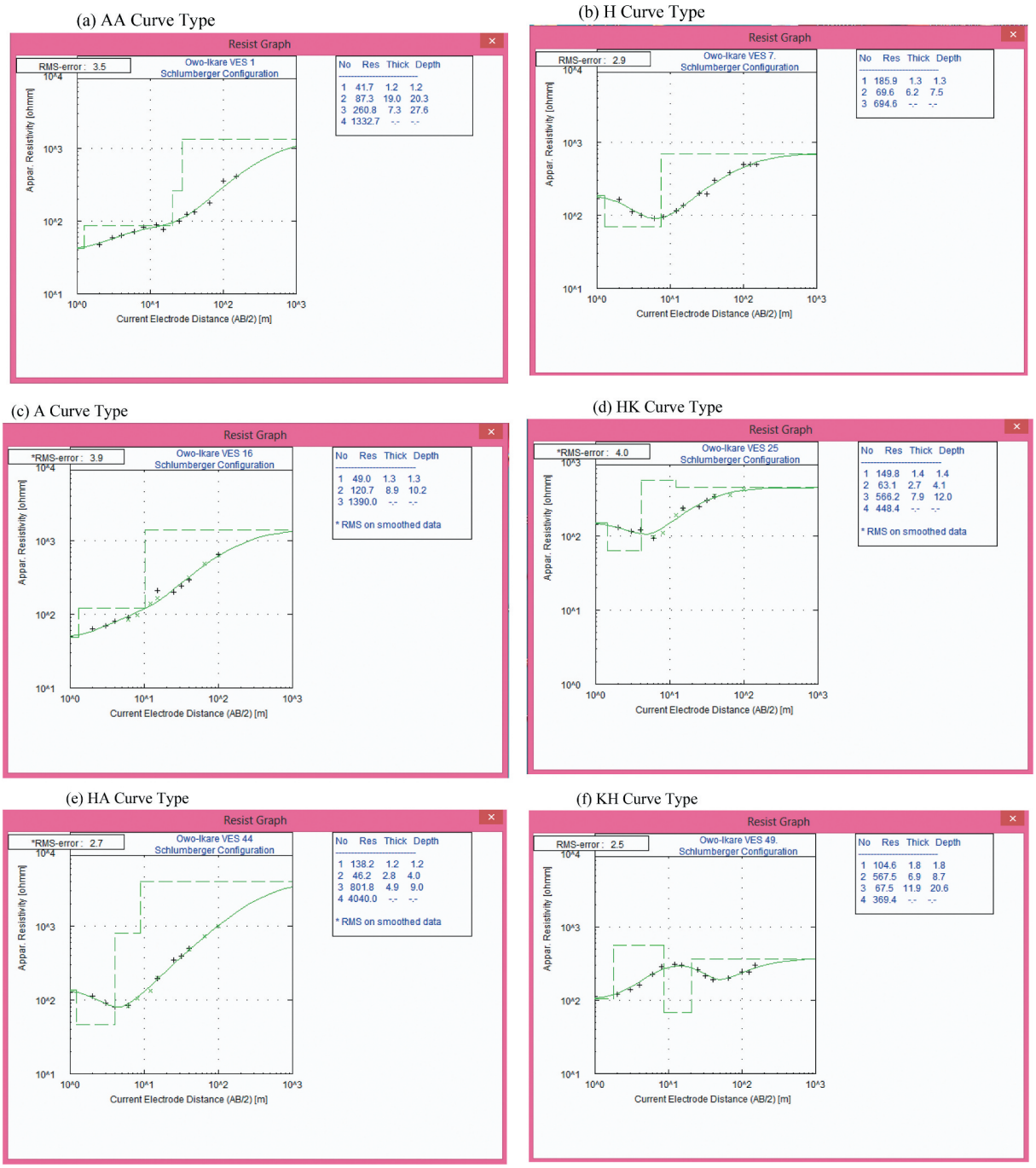

Figure 3. Representative curve types obtained from the geoelectrical data of owo-ikare highway area: (a) AA curve type; (b) H curve type; (c) A curve type; (d) HK curve type; (e) HA curve type and (f) KH curve type.

Table 1. Summary of interpretation of the VES.

VES Number	Layer	Resistivity (Ohm-m)	Thickness (m)	Depth (m)	Probable lithology	Curve type
1	1	42	1.2	1.2	Topsoil	AA
	2	87	19.0	20.3	Weathered basement (clay)	
	3	261	7.3	27.6	Partially weathered/Fractured basement (sand)	
	4	1333	-	-	Fresh bedrock	
2	1	49	1.4	1.4	Topsoil	HA
	2	32	3.5	4.9	Weathered basement (clay)	
	3	276	12.5	17.4	Partially weathered/Fractured basement (sand)	
	4	925	-	-	Fresh bedrock	
3	1	187	0.9	0.9	Topsoil	HA
	2	51	3.0	3.9	Weathered basement (clay)	
	3	230	12.5	16.4	Partially weathered/Fractured basement (sand)	
	4	1494	-	-	Fresh bedrock	
4	1	59	0.8	0.8	Topsoil	HA
	2	23	6.0	6.7	Weathered basement (clay)	
	3	1119	7.1	13.8	Fresh bedrock	
	4	3501	-	-	Fresh bedrock	
5	1	126	1.0	1.0	Topsoil	HA
	2	59	8.1	9.1	Weathered basement (clay)	
	3	290	10.2	19.3	Partially weathered/Fractured basement (sand)	
	4	2221	-	-	Fresh bedrock	
6	1	186	0.8	0.8	Topsoil	HA
	2	91	3.3	4.0	Weathered basement (clay)	
	3	251	21.9	26.0	Partially weathered/Fractured basement (sand)	
	4	977	-	-	Fresh bedrock	
7	1	186	1.3	1.3	Topsoil	H
	2	70	6.2	7.5	Weathered basement (clay)	
	3	695	-	-	Partially weathered/Fractured basement (sand)	
8	1	256	0.5	0.5	Topsoil	HA
	2	85	12.3	12.8	Weathered basement (clay)	
	3	459	11.3	24.0	Partially weathered/Fractured basement (sand)	
	4	4561	-	-	Fresh bedrock	
9	1	237	0.4	0.4	Topsoil	HA
	2	43	4.7	5.1	Weathered basement (clay)	
	3	335	9.4	14.5	Partially weathered/Fractured basement (sand)	
	4	1614	-	-	Fresh bedrock	
10	1	47	1.2	1.2	Topsoil	HA
	2	25	2.8	4.0	Weathered basement (sandy clay)	
	3	790	9.2	13.2	Partially weathered/Fractured basement (sand)	
	4	2478	-	-	Fresh bedrock	
11	1	99	0.9	0.9	Topsoil	HA
	2	72	4.6	5.5	Weathered basement (clay)	
	3	603	12.4	17.9	Partially weathered/Fractured basement (sand)	
	4	1626	-	-	Fresh bedrock	
12	1	123	2.1	2.1	Topsoil	HA
	2	99	28.7	30.8	Weathered basement (clay)	
	3	183	11.7	42.5	Partially weathered/Fractured basement (sandy clay)	
	4	758	-	-	Fresh bedrock	
13	1	192	3.6	3.6	Topsoil	HA
	2	63	5.8	9.4	Weathered basement (clay)	
	3	661	8.4	17.8	Partially weathered/Fractured basement (sand)	
	4	3465	-	-	Fresh bedrock	
14	1	206	0.6	0.6	Topsoil	HA
	2	69	19.1	19.7	Weathered basement (clay)	
	3	204	9.0	28.7	Partially weathered/Fractured basement (sand)	
	4	685	-	-	Partially weathered/Fractured basement (sand)	
15	1	256	2.4	2.4	Topsoil	HA
	2	60	12.1	14.5	Weathered basement (clay)	
	3	338	9.9	24.4	Partially weathered/Fractured basement (sand)	
	4	628	-	-	Partially weathered/Fractured basement (sand)	
16	1	49	1.3	1.3	Topsoil	A
	2	121	23.9	25.2	Weathered basement (sandy clay)	
	3	1390	-	-	Fresh bedrock	
17	1	64	3.9	3.9	Topsoil	A
	2	125	21.5	25.4	Weathered basement (sandy clay)	
	3	2011	-	-	Fresh bedrock	
18	1	54	4.5	4.5	Topsoil	A
	2	80	15.9	20.4	Weathered basement (clay)	
	3	2033	-	-	Fresh bedrock	
19	1	29	1.8	1.8	Topsoil	A
	2	114	11.3	13.0	Weathered basement (sandy clay)	
	3	886	-	-	Fresh bedrock	

(*Continued*)

Table 1. (Continued).

VES Number	Layer	Resistivity (Ohm-m)	Thickness (m)	Depth (m)	Probable lithology	Curve type
20	1	64	4.3	4.3	Topsoil	A
	2	208	3.5	7.7	Weathered basement (clayey sand)	
	3	1874	-	-	Fresh bedrock	
21	1	109	2.7	2.7	Topsoil	HA
	2	64	9.3	12.0	Weathered basement (clay)	
	3	236	8.0	20.0	Partially weathered/Fractured basement (sand)	
	4	649	-	-	Partially weathered/Fractured basement (sand)	
22	1	215	2.8	2.8	Topsoil	HA
	2	167	7.5	10.3	Weathered basement (sandy clay)	
	3	364	9.3	19.6	Partially weathered/Fractured basement (sand)	
	4	628	-	-	Partially weathered/Fractured basement (sand)	
23	1	137	1.7	1.7	Topsoil	HA
	2	76	7.7	9.4	Weathered basement (clay)	
	3	222	13.2	22.6	Partially weathered/Fractured basement (sand)	
	4	633	-	-	Partially weathered/Fractured basement (sand)	
24	1	28	7.6	7.6	Topsoil	A
	2	110	4.9	12.5	Weathered basement (sandy clay)	
	3	824	-	-	Fresh bedrock	
25	1	150	1.4	1.4	Topsoil	HK
	2	63	2.7	4.1	Weathered basement (clay)	
	3	566	7.9	12.0	Partially weathered/Fractured basement (sand)	
	4	448	-	-	Partially weathered/Fractured basement (sand)	
26	1	280	1.4	1.4	Topsoil	HA
	2	80	7.6	9.0	Weathered basement (clay)	
	3	469	7.7	16.6	Partially weathered/Fractured basement (sand)	
	4	895	-	-	Fresh bedrock	
27	1	565	0.8	0.8	Topsoil	HA
	2	72	3.9	4.7	Weathered basement (clay)	
	3	437	10.3	14.9	Partially weathered/Fractured basement (sand)	
	4	1047	-	-	Fresh bedrock	
28	1	282	1.3	1.3	Topsoil	HA
	2	55	2.9	4.2	Weathered basement (clay)	
	3	608	10.5	14.7	Partially weathered/Fractured basement (sand)	
	4	1353	-	-	Fresh bedrock	
29	1	86	1.6	1.6	Topsoil	A
	2	222	8.8	10.4	Weathered basement (clayey sand)	
	3	721	-	-	Partially weathered/Fractured basement (sand)	
30	1	35	1.1	1.1	Topsoil	KH
	2	411	5.4	6.6	Laterite	
	3	218	13.6	20.2	Weathered basement (clayey sand)	
	4	780	-	-	Partially weathered/Fractured basement (sand)	
31	1	261	1.6	1.6	Topsoil	HA
	2	53	4.4	5.9	Weathered basement (clay)	
	3	511	4.5	10.4	Partially weathered/Fractured basement (sand)	
	4	2634	-	-	Fresh bedrock	
32	1	160	0.8	0.8	Topsoil	HA
	2	68	5.2	6.0	Weathered basement (clay)	
	3	466	7.4	13.4	Partially weathered/Fractured basement (sand)	
	4	2898	-	-	Fresh bedrock	
33	1	162	2.0	2.0	Topsoil	HA
	2	64	4.6	6.7	Weathered basement (clay)	
	3	568	5.8	12.5	Partially weathered/Fractured basement (sand)	
	4	2142	-	-	Fresh bedrock	
34	1	287	0.9	0.9	Topsoil	HA
	2	31	2.2	3.2	Weathered basement (clay)	
	3	683	4.8	7.9	Partially weathered/Fractured basement (sand)	
	4	709	-	-	Partially weathered/Fractured basement (sand)	
35	1	126	2.0	2.0	Topsoil	HA
	2	98	4.2	6.2	Weathered basement (clay)	
	3	548	7.7	13.9	Partially weathered/Fractured basement (clayey sand)	
	4	1357	-	-	Fresh bedrock	
36	1	189	1.5	1.5	Topsoil	HA
	2	53	3.5	4.9	Weathered basement (clay)	
	3	677	7.2	12.1	Partially weathered/Fractured basement (sand)	
	4	1020	-	-	Fresh bedrock	
37	1	146	1.2	1.2	Topsoil	HA
	2	75	3.0	4.3	Weathered basement (clay)	
	3	611	8.2	12.5	Partially weathered/Fractured basement (sand)	
	4	1035	-	-	Fresh bedrock	
38	1	183	1.1	1.1	Topsoil	HA
	2	83	3.9	5.0	Weathered basement (clay)	
	3	597	8.6	13.6	Partially weathered/Fractured basement (sand)	
	4	974	-	-	Fresh bedrock	
39	1	346	2.7	2.7	Topsoil	HA
	2	58	4.7	7.4	Weathered basement (clay)	
	3	434	5.0	12.4	Partially weathered/Fractured basement (sand)	
	4	2179	-	-	Fresh bedrock	

(*Continued*)

Table 1. (Continued).

VES Number	Layer	Resistivity (Ohm-m)	Thickness (m)	Depth (m)	Probable lithology	Curve type
40	1	174	1.7	1.7	Topsoil	HA
	2	65	3.9	5.6	Weathered basement (clay)	
	3	470	6.5	12.1	Partially weathered/Fractured basement (sand)	
	4	1440	-	-	Fresh bedrock	
41	1	189	0.8	0.8	Topsoil	HA
	2	56	2.8	3.6	Weathered basement (clay)	
	3	647	7.4	11.0	Partially weathered/Fractured basement (sand)	
	4	1422	-	-	Fresh bedrock	
42	1	216	2.5	2.5	Topsoil	HA
	2	60	7.0	9.5	Weathered basement (clay)	
	3	492	6.1	15.5	Partially weathered/Fractured basement (sand)	
	4	3847	-	-	Fresh bedrock	
43	1	246	1.2	1.2	Topsoil	HA
	2	56	2.4	3.6	Weathered basement (clay)	
	3	814	8.5	12.0	Partially weathered/Fractured basement (sand)	
	4	1554	-	-	Fresh bedrock	
44	1	138	1.2	1.2	Topsoil	HA
	2	46	2.8	4.0	Weathered basement (clay)	
	3	802	4.9	9.0	Partially weathered/Fractured basement (sand)	
	4	4040	-	-	Fresh bedrock	
45	1	263	2.9	2.9	Topsoil	HA
	2	66	7.6	10.5	Weathered basement (clay)	
	3	466	6.5	17.1	Partially weathered/Fractured basement (sand)	
	4	737	-	-	Partially weathered/Fractured basement (sand)	
46	1	325	0.6	0.6	Topsoil	HA
	2	68	2.9	3.4	Weathered basement (clay)	
	3	353	15.4	18.8	Partially weathered/Fractured basement (sand)	
	4	605	-	-	Partially weathered/Fractured basement (sand)	
47	1	145	1.3	1.3	Topsoil	HA
	2	27	2.3	3.6	Weathered basement (clay)	
	3	627	6.0	9.6	Partially weathered/Fractured basement (sand)	
	4	2878	-	-	Fresh bedrock	
48	1	455	2.0	2.0	Topsoil	KH
	2	1069	6.0	8.0	Laterite	
	3	309	19.5	27.5	Weathered basement (clayey sand)	
	4	1232	-	-	Fresh bedrock	
49	1	105	1.8	1.8	Topsoil	KH
	2	568	6.9	8.7	Laterite	
	3	68	11.9	20.6	Weathered basement (clay)	
	4	369	-	-	Weathered basement (clayey sand)	
50	1	575	0.8	0.8	Topsoil	KH
	2	633	11.9	12.7	Laterite	
	3	233	14.2	26.9	Weathered basement (sandy clay)	
	4	4042	-	-	Fresh bedrock	
51	1	450	1.9	1.9	Topsoil	KH
	2	811	4.7	6.6	Laterite	
	3	330	19.5	26.1	Weathered basement (clayey sand)	
	4	1141	-	-	Fresh bedrock	
52	1	549	2.1	2.1	Topsoil	KH
	2	646	7.3	9.4	Laterite	
	3	252	18.1	27.5	Weathered basement (sandy clay)	
	4	1822	-	-	Fresh bedrock	
53	1	468	2.6	2.6	Topsoil	AA
	2	657	5.7	8.3	Laterite	
	3	1104	4.5	12.8	Fresh bedrock	
	4	2577	-	-	Fresh bedrock	
54	1	647	1.6	1.6	Topsoil	KH
	2	867	6.1	7.7	Laterite	
	3	354	6.0	13.7	Weathered basement (clayey sand)	
	4	2564	-	-	Fresh bedrock	

higher layer resistivity depicts higher competence and stability of subsoil. Processing and inversion of resistivity values from the 2-D electrical resistivity imaging were carried out with DIPROfWIN 4.01. This program computes an initial model and reduces the difference between the model and the field resistivity data until a satisfactory fit is obtained. The 2-D subsurface resistivity structures were interpreted with respect to subsurface lithology using the resistivity distribution, depending on the lateral and vertical continuity and geometry of the image responses as low continuous resistive subsurface substratum with resistivities <100 Ohm-m characterised by clay-rich material/water absorbing clayey layer/weathered basement, partially weathered/conductive fractured basement with resistivities

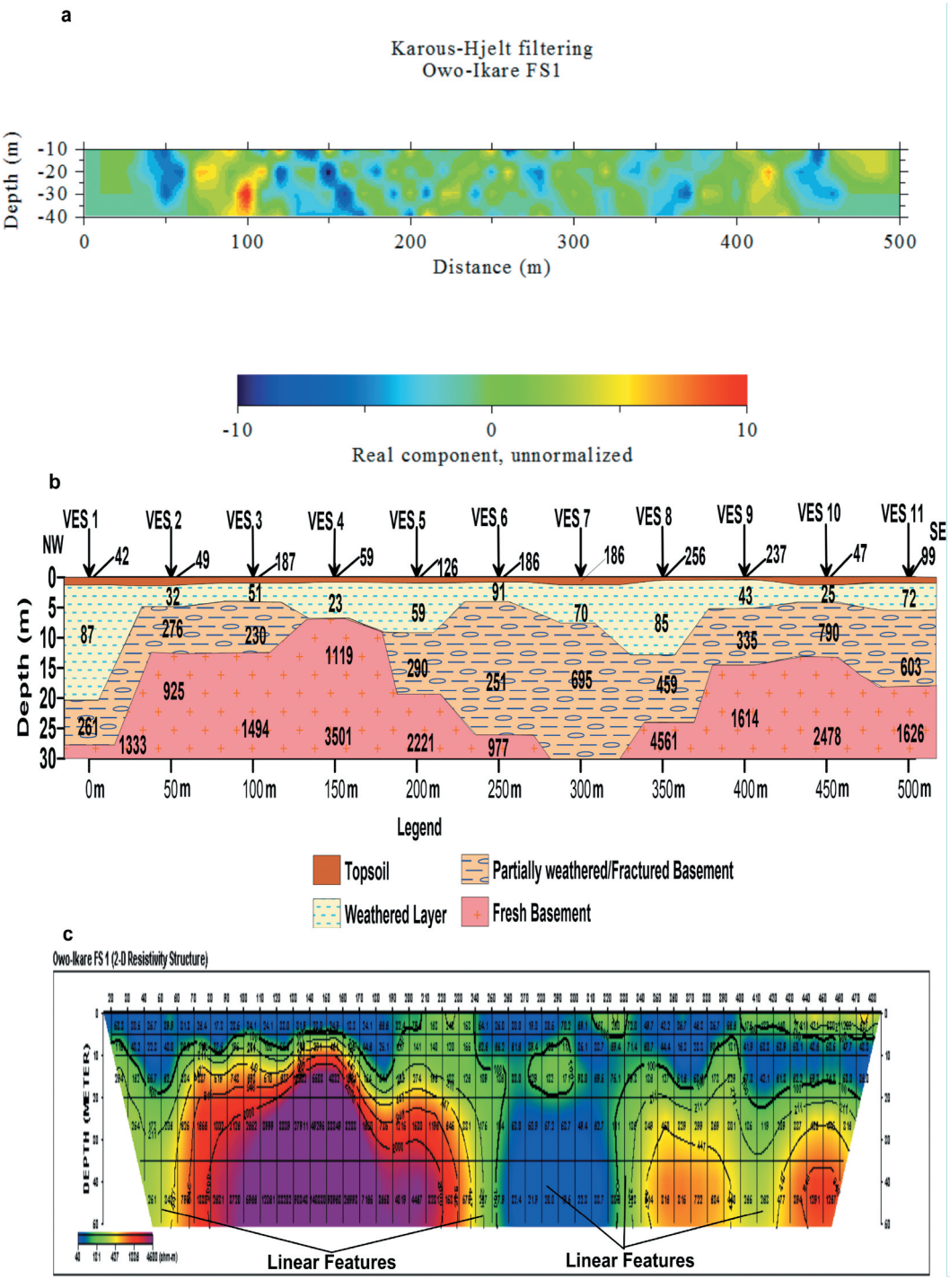

Figure 4. (a) VLF-EM 2-D inverted model, (b) geoelectrical section (c) two-dimensional (2-D) resistivity image of the subsurface of road .section 1

between 150 and 785 Ohm-m and high laterally and/or vertically continuous resistivities (>1000 Ohm-m) interpreted as fresh bedrock.

4.1.1. Location 1: owo (road section 1*)*

Conductive bodies cut across the failed section at distance 70–130 m and 200–500 m on VLF-EM section (Figure 4a). These conductive zones are possible fractures/faults, aquiferous zone or incompetent clayey zones beneath the subsurface. Four subsurface units consisting of topsoil, weathered basement, partially weathered/fractured basement and fresh bedrock were observed (Figure 4b). The resistivity values of the topsoil layer vary from 42 to 256 Ohm-m with layer thickness ranging 0.4–1.4 m. Most part of this topsoil is characterised by low resistivity below 100 Ohm-m. The topsoil in some places lies within the weathered basement because of its thickness and it's composed of clay, sandy clay and clayey sand. The resistivity of the clayey weathered layer varies from 23–91 Ohm-m with thickness in the range 1.7–19.0 m. This shows that the road pavement is constructed on water-saturated

subgrade soil characterised by clayey materials and indicative of incompetent formation influencing failure of the highway. The presence of clay facilitates failure of the road. Resistivity values of the partially weathered/fractured layer are in the range 230–790 Ohm-m with thickness in the range 2.1–21.9 m localised at all the VES points. The resistivity values indicate water-saturated fractured layer that pose threat to the road pavement. The resistivity values of the fresh bedrock are in the range 925–4561 Ωm with depth to bedrock from 7 m – 27.6 m. The bedrock topography is uneven with the overburden formation thickest at VES 1 (Figure 4b). Basement depressions observed at VES 1, 5 and 8 could also be another factor responsible for the road pavement instability. The 2-D subsurface resistivity structure (Figure 4c) shows clayey overburden of the section. It identifies low resistive linear features within the failed section at distance 0–20 m, 100–220 m, 320–420 m and 470–520 m. Some of these subsurface features reflect as high conductive features on the VLF-EM 2-D model (Figure 4a). These observed near-vertical features with depth extent (>10 m) indicative of the existence of fractures/faults and lithological contacts. Conductive structures observed on VLF-EM section at distance 350–430 m (Figure 4a) correspond with the bedrock depression at distance 330–380 m, fracture basement on the geoelectric section and also, the low resistive features on the 2-D resistivity structure at distance 230–430 m. Road pavement instability at this location is as a result of incompetent clayey subsoil, subsurface features suspected to be faults/fracture, aquiferous zone or lithological contact. These features serve as zones of weakness that accumulate water thereby reducing the strength of subsoil resulting to road pavement failure.

4.1.2. Location 2: oba-akoko (road section 2*)*

There are features of different degrees of conductivity on the section. Presence of high conductive zones at different points is indicative of weak/incompetent layer across the road section. Linear features displayed very high conductivity on VLF-EM section at surface distance of 60–125 m and 200–270 m suspected geologic features such as fault or fracture (Figure 5a). The top layer has resistivity values ranging from 49 to 256 Ωm (clay, sandy clay and clayey sand) with thickness in the range 0.6–4.5 m. VES stations 12, 14, 18 are the worst portions of the road with low resistive topsoil (49–123 Ωm) suggesting clayey topsoil with possibly high moisture content. The weathered basement beneath the topsoil has resistivity and thickness values ranging from 63–125 Ωm and 3.0–28.7 m in that order. Weathered basement predominantly clayey has resistivity values <130 Ohm-m (Figure 5b). Thus, the clayey layer is an incompetent engineering construction material that poses threat integrity/stability of the highway. Resistivity values of this layer indicate high level of saturation corresponding to aquiferous zone in the area, suggesting the reason the section of the road is extremely bad. This layer highlights low resistive features having high water content, suggesting fracture or buried stream channel. The resistivity values of partially weathered/fractured basement in the range 183–685 Ohm-m and thickness 8.4–11.7 m confined in VES stations 12–15. These values portray aquiferous zone beneath the subsurface that influence the instability of the highway. The resistivity values of the fresh bedrock vary from 958 to 3465 Ohm-m with uneven bedrock topography. However, the depth to bedrock varies from 6.9 – infinity. Bedrock depression is observed beneath VES 12 and 14 filled with very low resistivity facies which could contribute to road failure. The 2-D subsurface structure displays a low resistivity layer (< 60 Ohm-m) across the section and at the northwestern flank, there are suspected linear features within the failed section at distance of 90–150 m (Figure 5c). These subsurface features show high

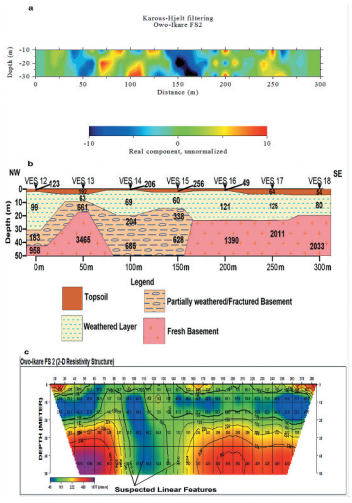

Figure 5. (a) VLF-EM 2-D inverted model, (b) geoelectrical section and (c) two-dimensional (2-D) resistivity image of the subsurface of road .section 2

conductivity on the 2-D model at distance of 70–125 m (Figure 5a). The observed features with depth >15 m suggest fractures and lithological contacts. Closures of weathered materials (<60 Ohm-m) observed in the resistive zones are typical of saturated clay materials and have adverse effect on stability of highway pavement.

4.1.3. Location 3: etioro-akoko (road section 3)

Subsurface conductive features are observed on the VLF-EM 2-D section in the failed section at stretch of 120–175 m along the road pavement (Figure 6a). The identified linear feature is an indication of geological features underlying the unstable section with specification of confined basement fracture beneath the road pavement. Four subsurface layers are delineated at this location (Figure 6b), resistivity of topsoil vary from 28 to 215 Ohm-m signifying clay and clayey units having thickness which varies between 1.4–7.6 m. It is observed from the geoelectric section that VES 19–23 (the extremely bad section of the road) are characterised with topsoil of low resistivity values

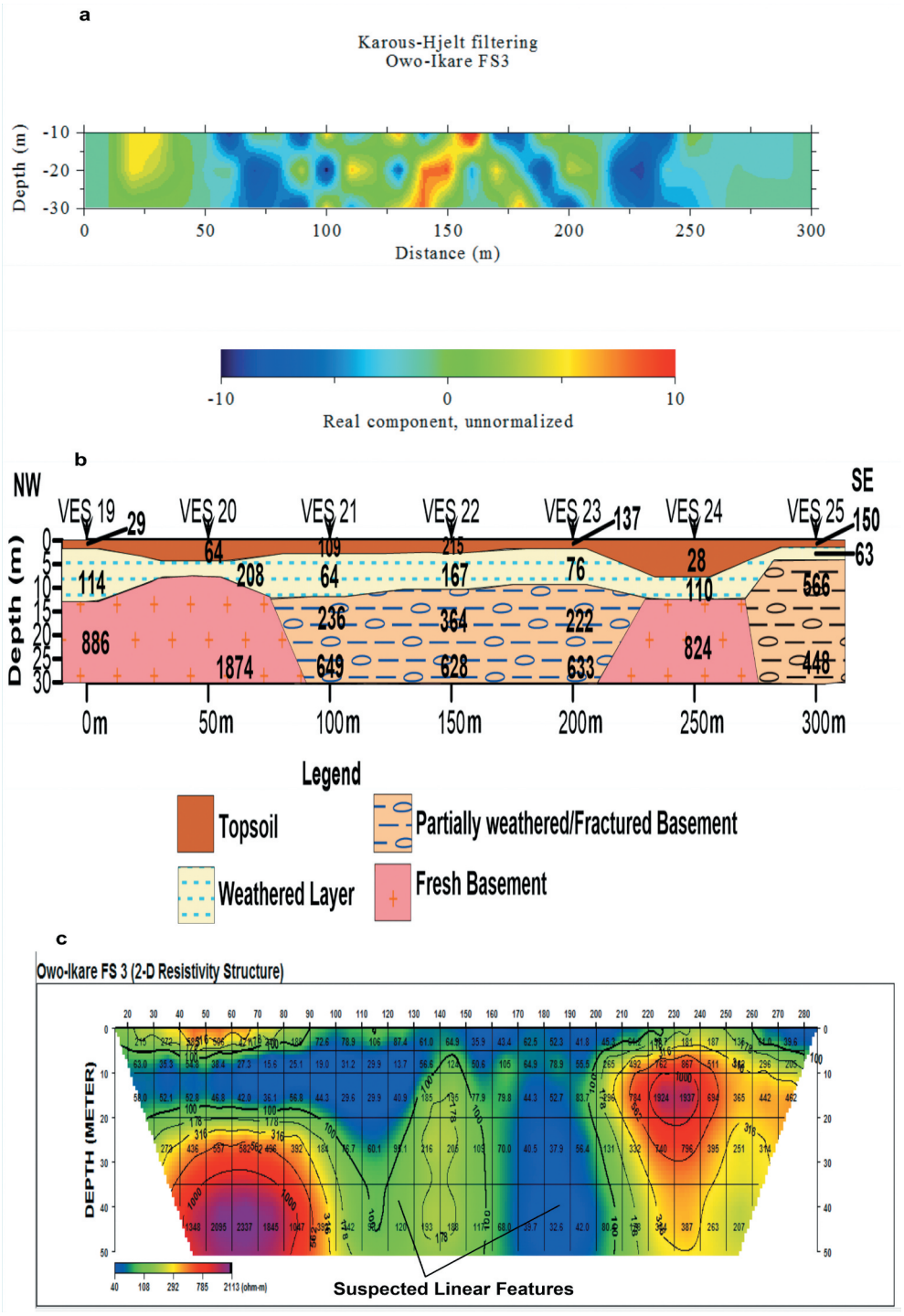

Figure 6. (a) VLF-EM 2-D inverted model, (b) geoelectrical section and (c) two-dimensional (2-D) resistivity image of the subsurface of Road .Section 3

of between 28 and 109 Ohm-m suggesting clayey topsoil with possibly high moisture content. The resistivity and thickness of weathered basement are in the range 63–208 Ohm-m and 3.5–11.3 m, respectively. Water saturated clay is dominant in the weathered zone due to its low resistivity values <100 ohm-m. Partially weathered/fractured layer, the third layer has resistivity values ranging 222–649 Ohm-m beneath VES stations 21, 22, 23 and 25. This range of resistivity corresponds to aquiferous zone beneath the subsurface that contribute to instability of the highway. Presence of this layer (saturated subgrade) constitutes weak zones that facilitate failure of the highway pavement. The last geoelectric substratum, the fresh bedrock has resistivity values varying from 824–1874 Ohm-m with depth to bedrock in the range 7.7 to over 30 m (Figure 6b). The 2-D subsurface structure showed three lithological units (topsoil, weathered basement and fresh bedrock) (Figure 6c). The topsoil subsumes into the weathered basement at distance 90–210 m due to its thickness and is characterised as clay enriched water absorbing substratum. The low resistivity values generally (<60 Ohm-m) indicate the presence of water-absorbing clay which precipitates instability of the highway pavement. It shows near vertical subsurface structures having low resistivity and significant depth > 40 m at surface distance expression of 150–200 m. This vertical

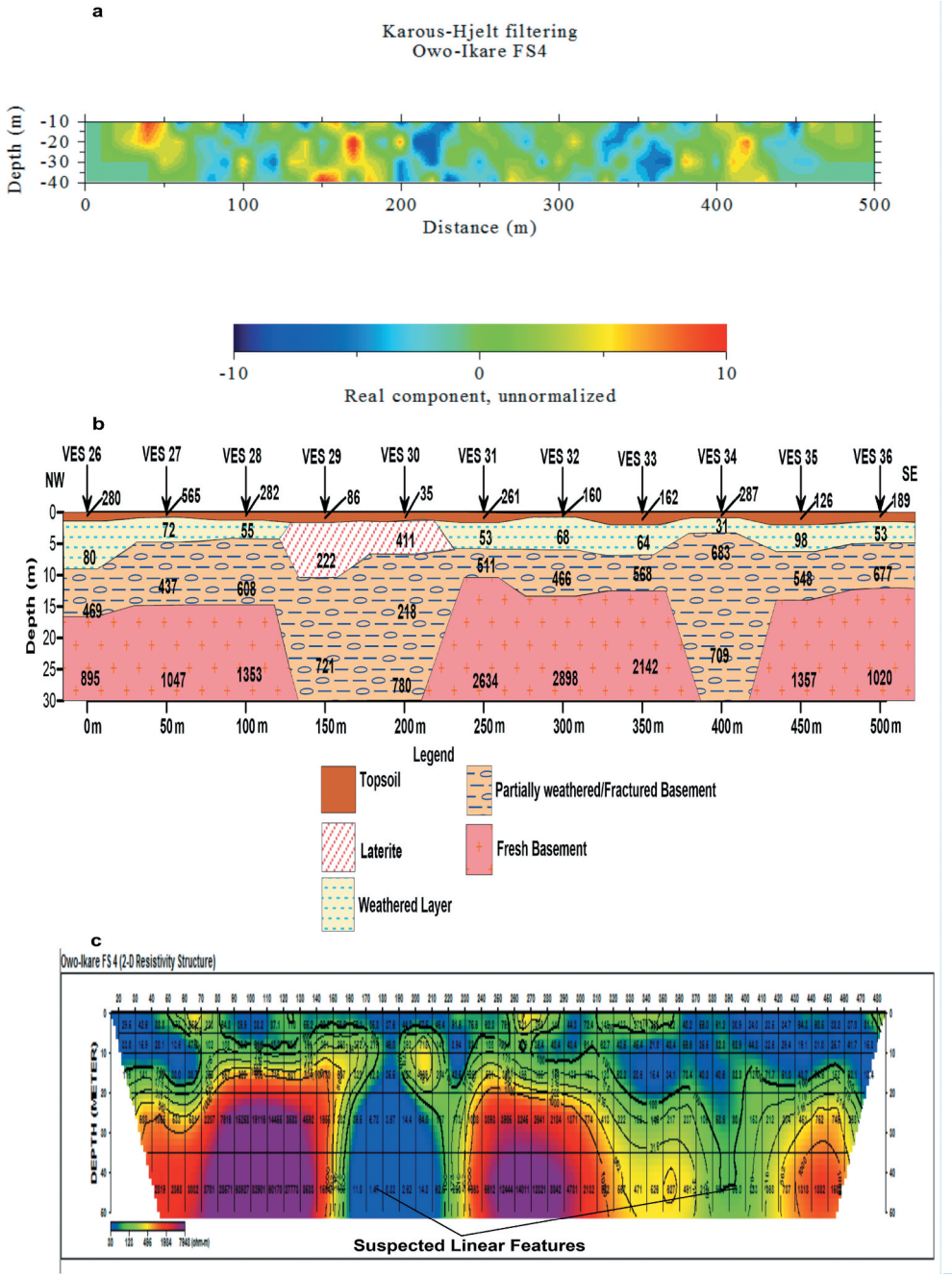

Figure 7. (a) VLF-EM 2-D inverted model, (b) geoelectrical section and (c) two-dimensional (2-D) resistivity image of the subsurface of road .section 4

discontinuity contributes to instability of the highway pavement and may likely affect the presently stable sections in the environment. Towards the southeastern flank, there is clayey sand/lateritic intrusion at surface distance expression of 210–260 m due to higher resistivity values >200 Ohm-m. Basement bedrock interface is uneven and dipping towards the northwest (Figures 6b and 6c). Combination of incompetent clayey subsoil, identified near-surface and subsurface structures; fractures, aquiferous zones and geological contact are contributing features causing instability of the highway pavement.

4.1.4. Location 4: akungba-akoko (road section 4)

The 2-D inverted model shows the existence of linear features of different degrees of conductivity at distances between 25–70 m, 100–220 m, 270–320 m and 380–500 m dipping NW – SE and NE – SW (Figure 7a). The presence of the near surface cross cutting linear features is indicative of weak/incompetent geologic formation upon which the road pavement was constructed, which accounts for its failure. Four subsurface layers are delineated at this location; the topsoil, weathered basement, partially weathered/fractured layer and fresh bedrock (Figure 7b). The resistivity values of the topsoil range from 35 to 565 Ohm-m (corresponding to clay and sand) with thickness 0.8–2.0 m. The topsoil falls into the weathered basement in some parts as a result of its thickness. There exist laterite beneath the topsoil having resistivity and thickness in the range 222–441 Ohm-m and 5.4–8.8 m, respectively, at VES 29 and 30. The

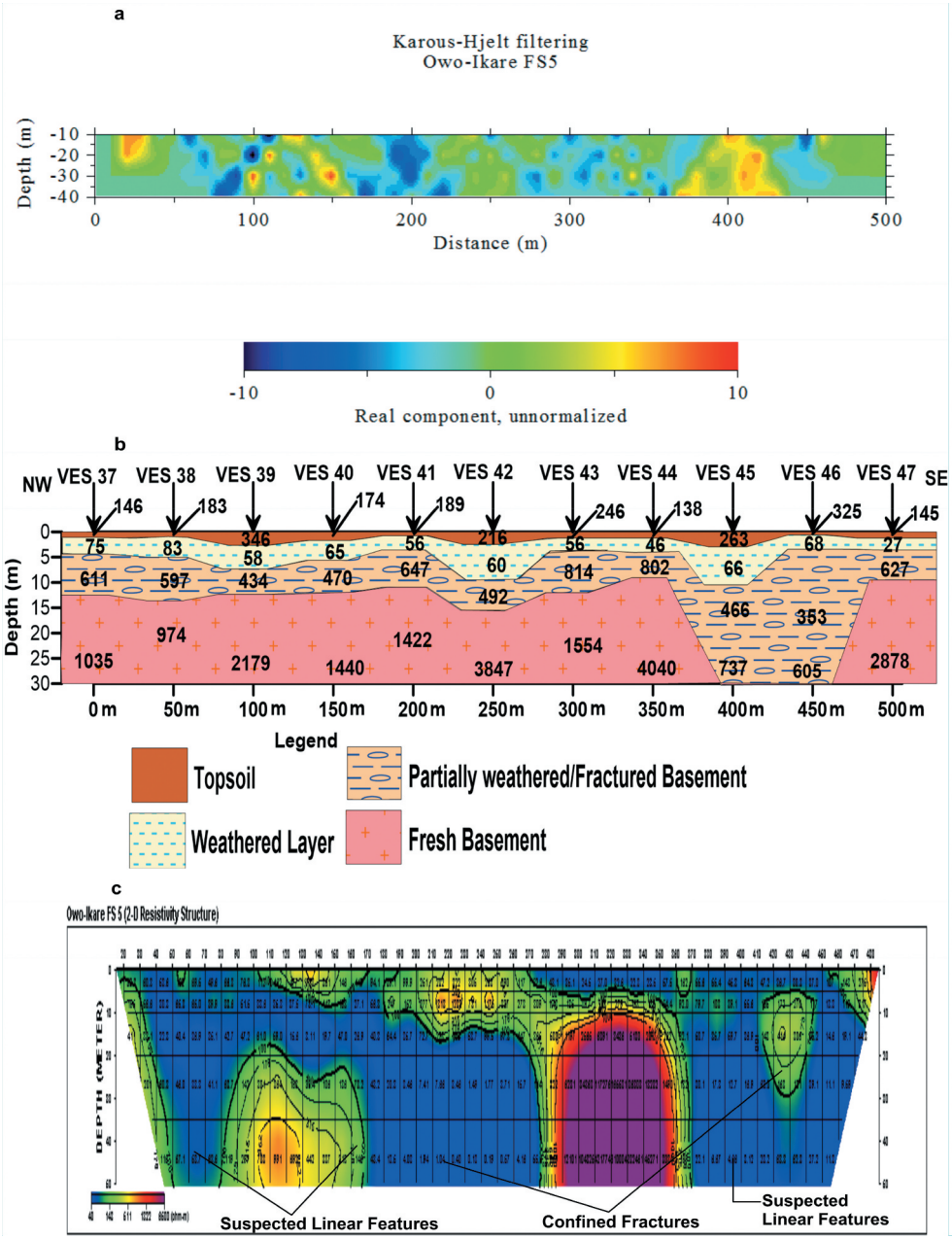

Figure 8. (a) VLF-EM 2-D inverted model, (b) geoelectrical section and (c) two-dimensional (2-D) resistivity image of the subsurface of road .section 5

weathered basement is clay with resistivity values varying 31–98 Ohm-m and layer thickness varying from 2.2 to 7.6 m. Areas with predominance of clay and depressions constitute civil engineering problematic sites. The clay composition of the weathered layer accounts for instability of the highway pavement. Third layer has resistivity values varying 218–780 Ohm-m. This range of resistivity depicts water-saturated zone beneath subsurface that contribute to instability of the highway. It is established that low resistivity (weathered regolith) thick overburden and fractured bedrock below the weathered layer constitute the aquifer units for groundwater development in the area (Oluwafemi and Oladunjoye 2013). The existence of this layer leads to reduction of subsoil strength of the road layers, which facilitates incessant failure of the highway pavement even shortly after rehabilitation and reconstruction. The last geoelectric substratum, fresh bedrock has resistivity values varying 895–2898 Ohm-m with depth to bedrock ranging 7.9 – above 30 m (Figure 7b). Clayey materials (low resistive zone) between the depth of 0–10 m are observed on the 2-D subsurface structure at surface distance 25–55 m, 80–110 m, 170–230 m, 360–480 m within the unstable section (Figure 7c). Deep weathering section at 160–210 m represents the fracture plane separating the fresh bedrock and fractured section at 370–420 m at this location. This deep weathering section possibly conducts groundwater at this location and signifies saturated clayey substratum. The identified distinct low resistive subsurface features with depth >40 m at 160–210 suspected to be faults within the bedrock. This confirms the weathered basement and fractured basement on geoelectric section of the location. The subsurface features shown on 2-D structure at 160–210 and 370–420 m correspond with the conductive features on VLF-EM section.

4.1.5. Location 5: ikare-akoko (road section 5)

Observed linear features display fairly high conductivity at surface distance of 100–180, 250–300 and 370–440 m, which are suspected faults and fractures (Figure 8a). Four subsurface layers are delineated at this location; the topsoil with resistivity and thickness values in the range 138–346 Ohm-m and 0.6–2.9 m signify clayey sand/laterite. Weathered layer beneath the top layer has resistivity and thickness values ranging from 27–83 Ohm-m and 2.3–7.6 m. Clay composition of the weathered layer with resistivity values <100 Ohm-m indicate saturated nature of the subsoil which precipitate failure of the road. This suggests that the road pavement is constructed on an incompetent (weathered) layer which accounts for the continuous failure along the road even shortly after maintenance and reconstruction works. The partially weathered/fractured basement has resistivity values varying from 353 to 814 Ohm-m. The resistivity values suggest aquiferous zone beneath subsurface that also contribute to the highway instability. Resistivity of the fresh bedrock varies from 974 to 4040 Ohm-m with infinite depth. The bedrock topography is uneven with depth to bedrock in the range 9.0 to over 30.0 m (Figure 8b). The 2-D resistivity structure showed low resistive geomaterials at some points above the depth of 30 m (Figure 8c). This suggests the existence of saturated clayey substratum (weathered zone) within the bedrock. It identifies linear features at distance 20–100 m, 150–180 m, 360–480 m and confined bedrock fractures at distance 180–280 and 410–450 m which fall within intensively fractured basement on the geoelectric section. These subsurface features show high conductivity on the 2-D VLF-EM model (Figure 8a). Highway pavement failure at this location is as a result of incompetent clayey subsoil, near-surface and subsurface linear features.

4.1.6. Location 6: owo (road section 6)

The VLF-EM 2-D inverted model is devoid of linear geological features (Figure 9a) such as fault, fracture, aquiferous zones and lithological contact which are zones of weakness that tend to reduce the load-bearing capacity/strength of the subsoil upon which the road pavement is constructed. Four subsurface layers are also delineated at this study location (Figure 9b). The topsoil is resistive with resistivity and thickness in the range 450–647 Ohm-m (sand/lateritic sand) and 0.8–4.5 m. Lithological unit below the topsoil has resistivity values varying from 568 to 1069 Ohm-m with the thickness varying from 4.7 to 11.9 m indicates lateritic sand along the road section thick enough to support the subsoil load-bearing capacity. The resistivity of the underlying thick weathered basement suggests majorly sandy facies. Existence of lateritic and resistive topmost layer accounts for the stability of this section of the highway (Figure 9b). High resistive weathered basement is as a result of the type of pre-existing parent rock (quartzite) in this location. Thus, geological condition of an area is a key factor for stability of roads. The resistivity of the fresh bedrock is in the range 1141–4042 Ohm-m, while depth to bedrock varies from 12.3 – over 30 m (Figure 9b). The results show that the unstable sections of the highway are composed of clay at depth lower than the stable section. The resistivity subsurface structure (Figure 9c) displays no evidence of subsurface geological structures that could precipitate failure of the road. This confirms the field observation as no distress was noticed on this section of the road. The bedrock topography (Figure 9b) also corroborates the VLF-EM inverted model (Figure 9a) and the 2-D resistivity structure that is devoid of subsurface feature, are indication of a near homogeneous subsurface sequence (Figure 9c).

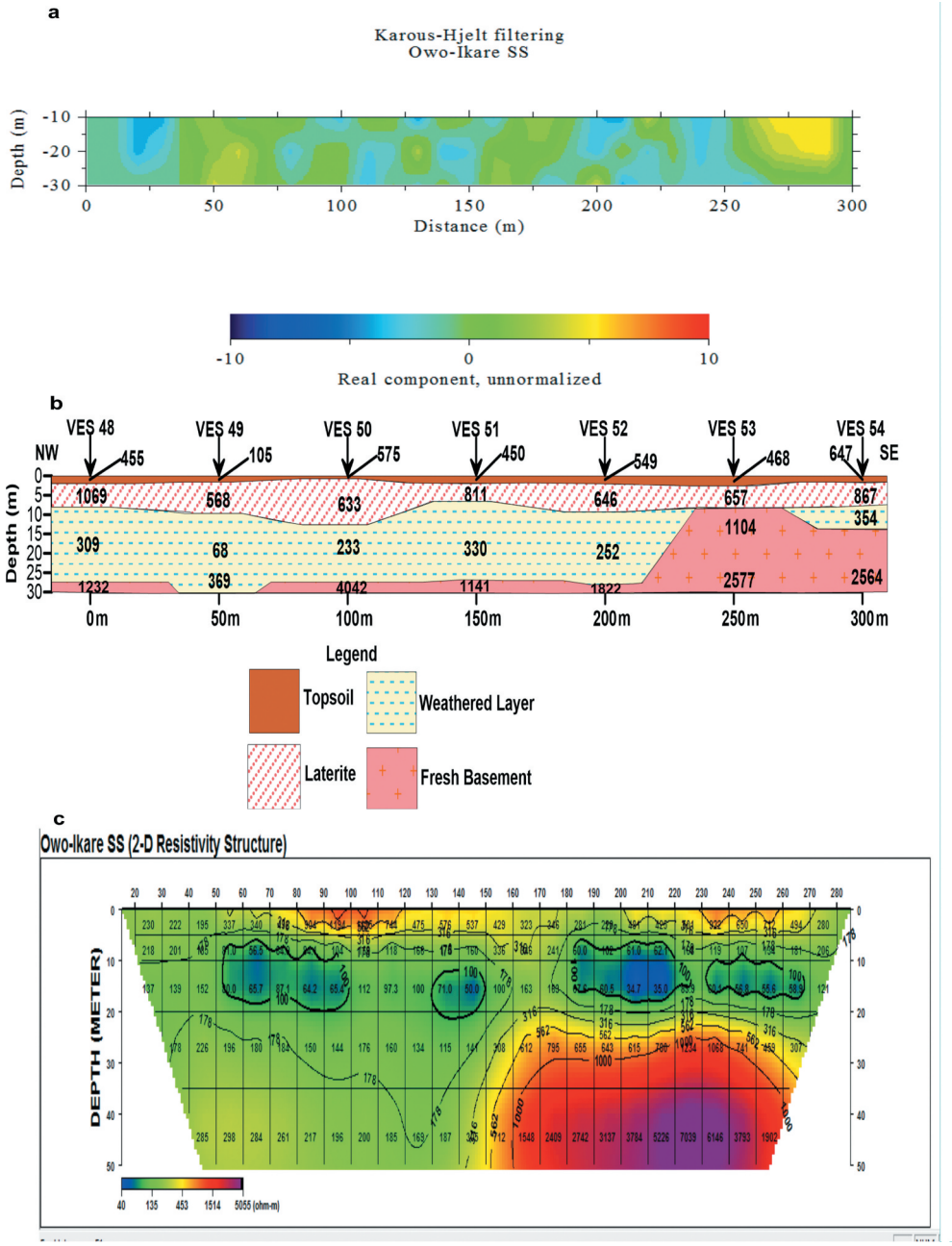

Figure 9. (a) VLF-EM 2-D inverted model, (b) geoelectrical section (c) two-dimensional (2-D) resistivity image of the subsurface of road section 6.

The results of the integrated geophysical surveys showed that the highway failure are due to the presence of low resistive geo-materials, deep weathering and fracturing of the bedrock (Table 2), geological features, irregular bedrock topography, bedrock depressions filled with low resistivity weathered materials, shallow water table, poor construction practices and absence of effective drainage system.

4.2. Geotechnical results

The geotechnical property results are summarised in Table 3–6. Soils of the unstable sections have natural moisture content range from 21.4 to 33.6%, while that of stable section is from 18.7 to 19.3%. The difference in these values could be as a result of hydrogeological factors of the location as moisture content gives an insight on the level of water in a location (Ademila 2019). The high moisture content values especially at the unstable sections suggest water migration to the pavement which causes lubrication of soil particles that makes the pore pressure in the absorbed film to push the soil particles apart and result to reduction of the particle interlock which reduces the strength of the pavement. The natural water content shows that the soils have affinity for water which has effects on its expansion and contraction capacity. Specific gravity (Gs) of the soil beneath the failed sections and stable section ranges from 2.44 to 2.90. The

Table 2. Subsurface layers and their corresponding VLF-EM and electrical resistivity responses.

		VLF-EM Responses		Electrical Resistivity Responses (Ωm)				
Location code	Condition of road	Raw real range (%)	Filtered real range (%)	Topsoil	Laterite	Weathered layer	Partially weathered/ Fractured basement	Fresh basement
US 1	Unstable	−7.9–19.0	−12.1–18.9	42–256		23–91	230–790	925–4561
US 2	Unstable	−7.4–22.0	−17.1–18.9	49–256		60–125	183–685	958–3465
US 3	Unstable	−7.4–19.7	−5.2–10.5	28–215		63–208	222–649	824 – 1874
US 4	Unstable	−16.4–14.9	−9.3–16.9	35–565	222–411	31–98	218–780	895–2898
US 5	Unstable	−6.1–16.2	−7.3–13.3	138–346		27–83	353–814	974–4040
SS	Stable	−6.3–6.8	−6.2–8.5	450–647	568–1069	68–369		1104–4042

Table 3. The soils index properties.

Location code	Depth (m)	Road condition	Pit No.	Gs	Particle size distribution		Consistency Limits		
					Clay-sized particles range (%)	Fines range (%)	Liquid limit range (%)	Plasticity index range (%)	Linear shrinkage range (%)
US 1	0.5–1.5	Unstable	1–3	2.67–2.74	33.6–41.0	51–56	46.7–51.3	23.2–25.2	10.1–14.3
US 2	0.5–1.5	Unstable	4–6	2.44–2.76	40.5–45.4	55–63	50.1–63.8	22.1–34.4	11.4–16.3
US 3	0.5–1.5	Unstable	7–9	2.77–2.90	40.4–44.8	62–67	43.6–57.9	13.4–19.0	12.1–14.3
US 4	0.5–1.5	Unstable	10–12	2.67–2.77	28.7–36.1	40–46	44.7–53.6	23.1–29.7	11.9–13.9
US 5	0.5–1.5	Unstable	13–15	2.66–2.74	40.6–42.8	55–61	57.4–61.7	30.1–33.8	11.4–13.3
SS	0.5–1.5	Stable	16–18	2.66–2.72	16.6–19.3	28–30	20.1–25.2	6.5–8.3	5.9–8.1

difference in the specific gravity values of the soils may be as a result of their mineralogy. The proportions of fines of soils of unstable sections are in the range 40–67% and 28–30% for stable section (Table 3). The clay and silt contents of soils of unstable sections are >50% except that of unstable road section 4. All the unstable sections soils are within American Association of State Highways and Transport Officials A-7-5 to A-7-6 group (AASHTO, 2007), classified as poor soil for road construction being clayey soil type by Federal Ministry of Works and Housing, Nigeria 2000. Soils of stable section are within the group A-2-4 with <35% fines and lesser amount of clay content (< 20%) suitable for road construction (Table 3). Thus, it is observed that developed pressures by the clayey soils precipitate the road failure (Ademila 2018). Low clay size fraction in soils of stable section might be due to high degree of laterisation. High proportion of clay and silt in subsoil beneath the unstable sections is a contributory factor to the road instability. The consistency limits were presented in Table 2, with liquid limit (W_L) and plasticity index (PI) of soils of unstable sections in the range 43.6–63.8% and 13.4–34.4%, respectively, while those from stable section range from 20.1–-25.2% and 6.5–8.3%, respectively (Table 3). The high values of W_L and PI are indicative of clayey nature of the soils with poor engineering properties. Higher the value of W_L and PI, poorer is the quality of the soils for engineering purposes. Thus, soils of the unstable sections serve as poor foundation materials in road construction. Soils of unstable sections with PI >12% implies their incompetence for road subgrade, subbase and base course with the high PI attributed to high clay content of the soils (28.7–45.4%) (Table 3). This high clay content is responsible for cohesiveness and plasticity of the soils. Soils of the unstable sections are within the medium-high plasticity portion of Casagrande's plasticity chart (Figure 10) while soils of stable section demonstrate low plasticity. The soils lie above A-line representing inorganic soils except soils of unstable road section 3 which lie below A-line representing silts and organic soils of medium/high plasticity. Soils of unstable sections are classified as inorganic clays having medium/high plasticity (CI-CH), while soils from Etioro-Akoko (unstable road section 3) represent inorganic silt (MI–MH) of medium/high plasticity (Table 4) according to Unified Soil Classification System (USCS). It is obvious that the subsoils of the unstable road sections possess high clay and silt contents. These soils with poor geotechnical properties are susceptible to alternating expansion and contraction, posing threat to highway stability and other civil engineering construction works erected on it (Ademila 2019). Stable section soils are classified in group SCL of the USCS, indicating good subgrade and subbase soils. The values of the linear shrinkage are >8% recommended by Madedor (1983) with the implication that the soils would pose threat to stability of the highway. The contributory factor to highway instability in this area of study is as a result of the developed pressures exhibited by the clayey soils. Qualitatively, application of the soils as subgrade involves determination of the group index as in Table 4 to further classify the soils. Although, all the soils have group index of less than 20, they are poor quality subgrade and subbase materials in pavement construction based on AASHTO, 2007

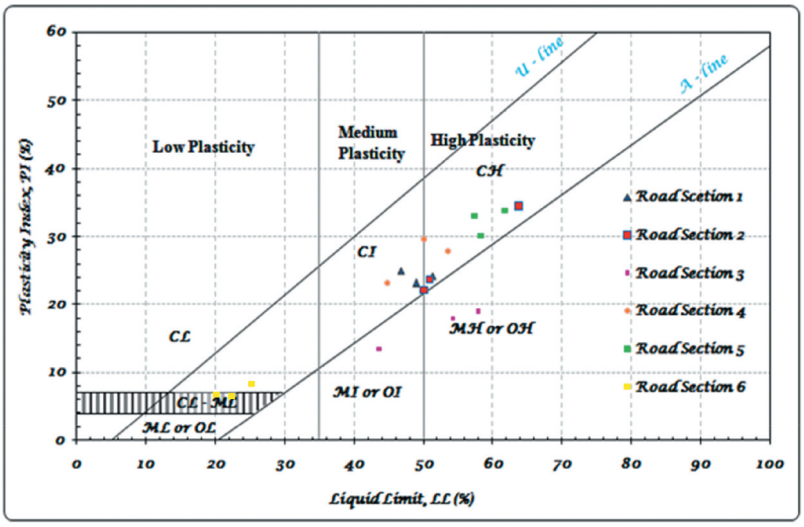

Figure 10. Casagrande plasticity chart of soils of unstable and stable sections.

Table 4. Soil classification of the study area.

Location code	Depth (m)	Road condition	Activity of clay	AASHTO Classification	Group Index, GI	USCS Classification	Soil type
US 1	0.5	Unstable	0.69	A-7-6	10	CI	Clayey
	1.0	Unstable	0.59	A-7-6	9	CH	
	1.5	Unstable	0.62	A-7-6	11	CI	
US 2	0.5	Unstable	0.52	A-7-6	14	CH	Clayey
	1.0	Unstable	0.85	A-7-6	16	CH	
	1.5	Unstable	0.54	A-7-6	12	CH	
US 3	0.5	Unstable	0.42	A-7-5	14	MH	Clayey
	1.0	Unstable	0.42	A-7-5	10	MH	
	1.5	Unstable	0.33	A-7-5	8	MI	
US 4	0.5	Unstable	0.97	A-7-6	9	CH	Clayey
	1.0	Unstable	1.03	A-7-6	6	CH	
	1.5	Unstable	0.64	A-7-6	6	CI	
US 5	0.5	Unstable	0.74	A-7-6	14	CH	Clayey
	1.0	Unstable	0.79	A-7-6	19	CH	
	1.5	Unstable	0.77	A-7-6	18	CH	
SS	0.5	Stable	0.50	A-2-4	0	SCL	Silty/clayey gravel and sand
	1.0	Stable	0.40	A-2-4	0	SCL	
	1.5	Stable	0.34	A-2-4	0	SCL	

and USCS classification systems. Activity, an index property used to determine the swelling potential of clay soils, i.e. the type of clay mineral present in soil and the possibility of the soil to exhibit colloidal behaviour that relates the mineralogical composition and geologic background of clays in the soils. Activity of the soils (A_c) derived from the failed sections are in the range 0.33–1.03 (Table 4). Most of these values are higher than those shown by kaolinitic clays (0.3 to 0.5) but they are all indicating the presence of normal soils (Holtz and Kovacs 1981) Soil classification based on activity value indicate <0.75 as inactive soil, 0.75–1.25 (normal soil) and >1.25 as active soil (Skempton 1953). The plot in the activity chart (Figure 11) shows that all the soils fall within the inactive and normal soils with kaolinite and illite as the dominant clay mineral in the soils having low-medium-high expansion characteristics.

SCL – Low Plasticity Clayey sand/Sand-clay mixture
CI – Medium Plasticity Clay
CH – High Plasticity Clay
MH – Silty Soil of High Plasticity
MI – Clayey Silt of Medium Plasticity

4.2.1. Strength characteristics

Soil resistance to deformation under load is a determinant of its strength (Das 2002) and poor geotechnical characteristics of soil pose by water can be minimised by compaction. The higher the maximum dry density (MDD) of soil at low optimum moisture content (OMC), the better for engineering purposes and stability under field conditions. MDD of soils of unstable and stable sections are in range 1532–1765 kg/m^3 and 1884–1920 kg/m^3 with OMC of 19.0–40.3% and 13.6–14.5% respectively (Table 5). These low values of MDD at high OMC suggest low bearing capacity of moist soils of the unstable sections. Dearth of effective drainage system in the area confirms high moisture content of the soils. The soils are prone to

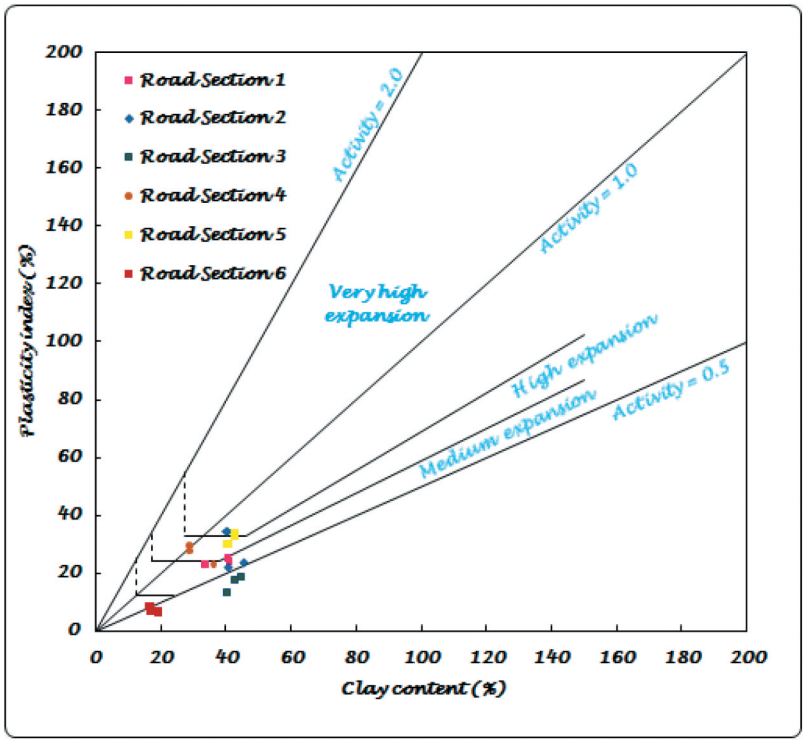

Figure 11. Activity chart of soils of unstable and stable sections.

Table 5. Strength characteristics of the soils.

Location	Soil Compaction		CBR		Triaxial Compression	
	MDD range (kg/m^3)	OMC range (%)	Unsoaked CBR range (%)	Soaked CBR (%)	Cohesion (kN/m^2)	Angle of Internal Friction (°)
US 1	1549–1586	26–27	7–10	3	77–93	27–33
US 2	1695–1765	26–31	23–36	16–26	73–95	27–33
US 3	1621–1741	19–40	23–28	16–19	85–86	29–31
US 4	1695–1722	19–20	34–38	23–27	78–90	24–33
US 5	1532–1572	26–28	17–19	5–6	79–88	29–30
SS	1884–1920	14–15	40–42	29–30	91–97	27–28

erosion due to their compaction characteristics. Unsoaked and soaked CBR values of soils of unstable sections are in the range7 – 38% and 3–27%, these values imply low load-bearing capacity of the soils (Table 5). Soaked CBR replicates condition of soil in excess water. The values show that the soils are vulnerable to volumetric changes on contact with water which results to highway instability as a result of its incapability to sustain imposed wheel stress. Minimum CBR values proposed for base course, subbase and subgrade are 80% unsoaked, 30% soaked and 10% soaked (FMWH, 2000). The soil sample of the stable section (SS/L1) only out of all the samples has the required minimum 30% soaked CBR but not the 80% minimum unsoaked CBR value that is recommended for highway subbase and base course. Soils beneath stable section demonstrate relatively higher strength and load-bearing capacity than the soils beneath failed sections. The poor geotechnical characteristics exhibited by the soils classifies them as incompetent for road construction. Cohesion ranges from 73–97 kN/m^2 for soils of the failed and stable sections. The angle of friction ranges from 24° to 33° for the soils (Table 5). The values of cohesion and angle of friction show moderate shearing strength of the soils. The soils of unstable sections have coefficient of volume compressibility (Mv) in the range 0.15–0.35 kN/m^2 (Table 6). Volume change characteristics of the

Table 6. Consolidation and permeability of the soils.

Location	Consolidation		Permeability, κ (cm/s)
	Coefficient of volume compressibility, Mv (kN/m^2)	Coefficient of consolidation, Cv (m^2/year)	
US 1	0.20–0.21	0.01–0.02	3.85×10^{-6} – 2.16×10^{-5}
US 2	0.20–0.34	0.01–0.02	1.83×10^{-6} – 2.57×10^{-6}
US 3	0.15–0.29	0.01–0.02	3.37×10^{-6} – 2.70×10^{-5}
US 4	0.26–0.32	0.01	1.71×10^{-6} – 3.99×10^{-6}
US 5	0.33–0.35	0.02	3.11×10^{-7} – 3.38×10^{-7}
SS	0.11–0.12	0.01–0.02	1.02×10^{-4} – 1.04×10^{-4}

soils indicate considerable differential settling for engineering construction works. Coefficient of consolidation, Cv of soils of unstable and stable sections are 0.01–0.02 m^2/year, while their permeability is in the range 3.11×10^{-7} – 2.70×10^{-5} cm/s and 1.02×10^{-4} cm/s to 1.04×10^{-4} cm/s (Table 6). This is an indication of impervious soils (clay and silt) hence, exhibiting water retention capability with declined strength. The distress observed in the failed sections would probably persist with time due to low permeability coefficient of the subsoil beneath the road pavement. Soils of some parts of the highway wear away due to non-existence of drainage, therefore effective drainage systems should be provided along the highway. Road design or construction planning should include appropriate drainage channels.

From engineering appraisal, unstable sections of the road are underlain by migmatite gneiss and biotite hornblende gneiss. The rock type is liable to weathering into clays and sandy clays/clayey sands. The subgrade of unstable highway sections is characterised by low resistive clayey soils (<100 Ohm-m). Thus, the failure along the sections of the road is precipitated by the clayey subsoil. The stable section is underlain by quartzite. The subgrade soil is lateritic, considerably thick enough (up to 11.9 m) to support imposed vehicular load. The geologic material being derived from quartzite is permeable, without water accumulation of the road structure. Clayey nature of the soil, subsurface structures, near-surface aquiferous zones delineated beneath the failed sections, geological condition and absence of drainage system account for the persistent failure of the road.

5. Conclusion

Subsurface investigation involving combined geophysical and geotechnical techniques were carried out to establish reasons for persistent instability of Owo-Ikare road. This study was with a view to determining the geological basis for highway failure in the area and serve as reference to other typical basement complex areas. It also intends to proffer lasting remediation measures to safe lives and valuables lost in accidents due to bad roads. VLF–EM survey was carried out along the failed and stable road sections, where real and imaginary components were measured. The real component data were thereafter processed. Data were filtered to enhance the signal in order to make tilt-angle crossovers easier to identify. The VLF–EM results were presented as inverted pseudosections. Fifty-four (54) Schlumberger sounding stations and electrical resistivity imaging using dipole-dipole configuration were employed along the failed and stable road sections.The VLF-EM 2-D inverted models revealed conductive zones at some locations suggesting weak zones responsible for structural instability. The identified conductive zones from VLF–EM survey are characteristics weak zones within the subsurface. These conductive zones are possible fractures/faults, aquiferous zone or incompetent clayey zones beneath the subsurface which facilitate the failure of the road. Maximum of four subsurface geoelectric/geologic layers were delineated with six different type of curves; H, AA, A, KH, HA and HK curve types from the geoelectric sections obtained from the interpreted vertical electrical sounding curves. This provides detailed insight into the subsurface structural disposition of the study area. The 2-D subsurface resistivity structures revealed clayey overburden and low resistive linear features within the failed road sections, which precipitate its failure. The results of the combined geophysical investigation show the presence of subsurface geological features beneath the road pavement which are structurally weak zones that constitute failure along the road. Saturated low resistive (<100 Ohm-m) clayey topsoil and weathered basement (subgrade) beneath the highway are characterised as poor subgrade and subbase construction materials with low strength/load-bearing capacity which contributes to the highway instability. Uneven bedrock topography coupled with depressions, fracturing and deep weathering of the bedrock which constitutes water-bearing unit beneath the subsurface pose threat to stability of the highway. Geotechnical results confirm the clayey nature of subsoil beneath the highway. Cohesiveness and plasticity of high clay and silt contents of the subsoil account for instability of the highway. These soils in AASHTO classification are in A-7-5 and A-7-6 group, classified as incompetent for road construction being clayey soil. Developed pressures and poor geotechnical characteristics exhibited by the subsoils also precipitate the road failure. Volume change characteristics of the soils could pose threat of considerable differential settlement in highway construction. Permeability of the soils classifies them as impervious; thus, they exhibit water retention capability with declined strength. Effective drainage system would avert water accumulation of the highway subsurface layers. Subsurface weak zones with geological structures and bedrock depressions should be consolidated. Also, soils beneath the unstable sections should be replaced with suitable soil during reconstruction for stability of the highway structures. Pavement design should be improved to include geologic condition, bedrock topography, subsurface structures and detailed

description of weather conditions. Information derived from this study is important for pavement design, rehabilitation, reconstruction of failed roads and sustainability of new roads. It also serves as a useful guide in road construction.

Acknowledgements

The author would like to thank the anonymous reviewers for their constructive comments and scientific remarks, which has improved the quality of this paper.

Disclosure statement

No potential conflict of interest was reported by the author.

ORCID

Omowumi Ademila http://orcid.org/0000-0001-5177-1110

References

Ademila O. 2015. Integrated geophysical survey for post foundation studies in a typical basement complex of southwestern nigeria. The Pacific Journal of Science and Technology. 16(2):274–285.

Ademila O. 2017. Engineering evaluation of lateritic soils of failed highway sections in Southwestern Nigeria. Geosciences Research. 2(3):210–218. doi:10.22606/gr.2017.23006.

Ademila O. 2018. Geotechnical influence of underlying soils to pavement failure in Southwestern part of Nigeria. Malaysian Journal of Sustainable Environment. 4 (2):19–36. doi:10.24191/myse.v4i1.5604.

Ademila O. 2019. Geotechnical properties and effects of palm kernel shell ash and cement on residual soils in pavement construction along owo-ikare road, Southwestern Nigeria. The Pacific Journal of Science and Technology. 20(1):365–381.

Ademila O, Olayinka AI, Oladunjoye MA. 2020. Land satellite imagery and integrated geophysical investigations of highway pavement instability in Southwestern Nigeria. Geology. Geophysics and Environment. 46(2):135–157. doi:10.7494/geol.2020.46.2.135.

Adeyemi GO, Oyeyemi F. 2000. Geotechnical basis for failure of sections of the Lagos-Ibadan expressway, Southwestern Nigeria. Bulletin of Engineering Geology and Environment. 59(1):39–45. doi:10.1007/s100649900016.

American Association of State Highway and Transportation Officials (AASHTO), 2007. Standard specifications for transportation materials and methods of sampling and testing. 27th Edition. Washington DC (USA): American Association of State Highway and Transportation Officials.

ASTM D4318. 2017. Standard test methods for liquid limit, plastic limit and plasticity index of soils. PA:American Society for Testing and Materials, ASTM International, West Conshohocken.

ASTM Standard D1557. 2009. Standard test methods for laboratory compaction characteristics of soil using modified effort. PA:American Society forTesting and Materials (ASTM) International West Conshohocken.

British Standard (BS) 1377, 1990. Methods of testing soils for civil engineering purposes. London:British Standards Institution.

Das BM. 2002. Principles of geotechnical engineering. Brooks/Cole. Pacific Grove (CA): 105. ISBN 0-534-38742–X.

Dipro for Windows. 2001. DiproTM Version 4.01. Daejon (South Korea):Processing and interpretation software for electrical resistivity data. Korea Institute of Geosciences and Mineral Resources (KIGAM).

Nigerian Federal Ministry of Works and Housing, Nigeria 2000. General specification for roads and bridges. Vol. 2. p. 137–275.

Holtz RD, Kovacs WD. 1981. An introduction to geotechnical engineering. New Jersey: Prentice Hall Inc., Engleword Cliffs.

Keller GV, Frischknecht FC. 1966. Electrical methods in geophysical prospecting. Oxford (UK): Pergamon Press Inc.; p. 523.

Koefoed O. 1979. Geosounding Principles. Netherlands: Resistivity sounding measurements. Elsevier Scientific Publishing Company Amsterdam. Vol. 1 p.275.

Madedor AC. 1983. Pavement design guidelines and practice for different geological area in Nigeria. In: Ola SA, editor. Tropical soils of Nigeria in engineering practice. A.A. Balkema. Netherland. 291-297

Olayinka AI, Oladunjoye MA, Osinowo OO, Adeyemi GO (2007). Integrated geophysical investigation to determine causes of structural failures at a factory site in Benin City, Nigeria. EAGE 69th Conference and Exhibition, London, UK. 11–14.

Oluwafemi O, Oladunjoye MA. 2013. Integration of surface electrical and electromagnetic prospecting methods for mapping overburden structures in Akungba-Akoko, Southwestern Nigeria. International Journal of Science and Technology. 2(1):122–147.

Orellana E, Mooney HM. 1966. Master tables and curves for vertical electrical sounding over layered structures. Madrid: Inteciencis; p. 34.

Pirttijarvi M. 2004. KH filt program. A geophysical software for karous-hjelt and fraser filtering on geophysical vlf (very low frequency) data. Geophysical division. In: Department of Geosciences. Finland: University of Oulu.

Rahaman MA. 1989. Review of the basement geology of Southwestern Nigeria. In: Kogbe CA, editor. Geology of Nigeria. Nigeria: Elizabeth Publishing; p. 39–56.

Skempton AW (1953): The colloidal activity of clays. In: Proceedings of the 3rd international conference on soil mechanics and foundation engineering, Zurich, Switzerland, Vol. 1: 57–61.

Telford WM, Geldart LP, Sheriff RE, Keys DA. 1990. Applied Geophysics. 2nd ed ed. Cambridge: Cambridge University Press; p. 344–536.

Vander Velper BPA. 2004. WinResist version 1.0 resistivity depth sounding interpretation software. ITC (Delft Netherland): M.Sc. Research Project.

Zohdy AAR. 1965. The auxiliary point method of electrical sounding interpretation and its relationship to Dar-Zarrouk parameters. Geophysics. 30(4):644–650. doi:10.1190/1.1439636.